Photochemical & Photobiological Sciences

Accepted Manuscript

This is an *Accepted Manuscript*, which has been through the Royal Society of Chemistry peer review process and has been accepted for publication.

Accepted Manuscripts are published online shortly after acceptance, before technical editing, formatting and proof reading. Using this free service, authors can make their results available to the community, in citable form, before we publish the edited article. We will replace this *Accepted Manuscript* with the edited and formatted *Advance Article* as soon as it is available.

You can find more information about *Accepted Manuscripts* in the Information for Authors.

Please note that technical editing may introduce minor changes to the text and/or graphics, which may alter content. The journal's standard Terms & Conditions and the Ethical guidelines still apply. In no event shall the Royal Society of Chemistry be held responsible for any errors or omissions in this *Accepted Manuscript* or any consequences arising from the use of any information it contains.

ROYAL SOCIETY OF CHEMISTRY

www.rsc.org/pps

Cite this: DOI: 10.1039/c0xx00000x

www.rsc.org/xxxxxx

ARTICLE TYPE

Synthesis of Thyminyl Stilbazoles and Their Photo-reactivity

Priscilla Johnston, Yuki Nishikami, and Kei Saito*

Received (in XXX, XXX) Xth XXXXXXXXX 20XX, Accepted Xth XXXXXXXXX 20XX

DOI: 10.1039/b000000x

Photo-reactions of molecules with two [2π+2π]-cycloaddition sites in the solid state are reported. Four thyminyl stilbazoles having both a stilbazole olefin and a thyminyl olefin were synthesized using the Heck reaction of halo-pyridine substrates with vinylbenzyl thymine or methylated vinylbenzylthymine. Only one of them, methylated vinylbenzylthymine with 4-pyridine was photoreactive and formed a head-to-tail stilbazole dimer. The crystal structures of thyminyl stilbazoles and the stilbazole dimer were used to investigate the structure-reactivity relationships.

Introduction

Topochemical reactions are increasingly being investigated as solvent free green reactions for the synthesis of complex molecules with controlled regio- and stereospecificity.[1,2] One of the topochemical reactions, solid state [2π+2π]-cycloaddition, involves a photo-chemical reaction between two olefinic molecules to yield a cyclobutane derivative.[3,4] Green synthetic routes to cyclobutane compounds are important since cyclobutane moieties occur in a number of natural products and alkaloids.[5] However, reports of molecules synthesised by the [2π+2π]-cycloaddition are limited. It is challenging to design new molecules for [2π+2π]-cycloaddition as the reactive molecules must be suitably positioned/oriented within the crystal lattice. Schmidt's topochemical postulate states that for a solid-state [2π+2π]-cycloaddition reaction to occur, the pair of reactive olefins should be parallel to one another, and be separated by a distance of 3.5-4.2 Å.[6] Schmidt also explained that the photo-dimerisation reactions occurred with a minimum amount of molecular movement, which means that the topochemistry of the reactant molecules is directly related to the stereochemistry of the resulting photo-product molecules. With few exceptions,[7] Schmidt's topochemical arguments concerning the reactivity of crystalline solids hold true to this day.

Stilbazole derivatives are known to form dimers by [2π+2π]-cycloaddition and a number of literature examples are reported which focus on their dimerization in the solid state, with and without template molecules.[8-12] Thymine, one of the nucleobases in DNA, is also known to undergo [2π+2π]-cycloaddition.[3,13-15] Photo-dimerization of thymines is known to disrupt the helical structure of DNA, leading to formation of DNA lesions.[16] The lesions create isolated loops in the DNA strand which causes loss of genetic information during subsequent cellular-replication cycles. For this reason, thymine dimerization is implicated as the cause of certain skin cancers.[17] It is therefore important to study thymine dimerizations to understand this phenomenon.

In this paper, we have synthesized thyminyl stilbazoles which possess both a stilbazole olefin and a thyminyl olefin in their structure. These molecules have a potential to form five different types of products via [2π+2π]-cycloaddition (**Figure 1**). They can form a stilbazole dimer from the cycloaddition of the stilbazole olefins, they could form a thyminyl cyclobutane dimer from the cycloaddition of the thyminyl olefins, or an asymmetric dimer from cycloaddition between the thyminyl and stilbazole olefin. A symmetric or asymmetric polymer could also be formed when both the stilbazole and thyminyl olefins dimerize.

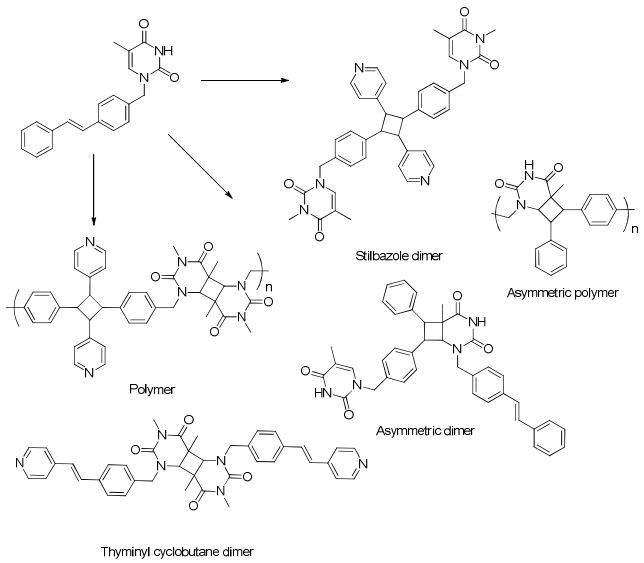

Figure 1. Possible photo-products from the irradiation of thyminyl stilbazoles.

The photo-activity of these synthesized thyminyl stilbazoles was studied to investigate the photo-product. In addition, the crystal packing of molecules was studied to understand the structural factors necessary to achieve adequate topochemistry and to

explain in detail why certain molecular features lead to a certain photo-product.

Experimental

Materials and methods

All chemicals were purchased from Sigma-Aldrich, Castle Hill, NSW, Australia. Solvents were purchased from Merck, Kilsyth, Victoria, Australia. Microwave syntheses were carried out using a CEM-Discover instrument in either 10 mL or 35 mL vials. A dynamic method was used in which the maximum pressure and power settings were 300 psi and 300 W, respectively. Melting points were determined using a Buchi B-545 melting point apparatus with a digital thermometer. IR spectra were recorded by using a Bruker Equinox 55 in ATR mode with diamond as the background reference. ^{1}H NMR spectra were recorded at 400 MHz on a Bruker DPX-400 spectrometer. ^{13}C NMR spectra were recorded at 100 MHz on a Bruker DPX-400 spectrometer. Electrospray ionisation mass spectra (ESI) were recorded on a Micromass platform II API QMS Electrospray mass spectrometer.

Single crystals (SC-XRD)

All structural analyses were performed on the MX1 micro-crystallography beam-line at the Australian Synchrotron, Clayton, Victoria. The end station comprised a φ goniostat with a Quantum 210r area detector. Data were collected using the Blue Ice GUI and processed using the XDS software. CCDC depositions 984307, 984308, 984309, 984310, and 984311 contain the supplementary crystallographic data for this paper. These data can be obtained free of charge from The Cambridge Crystallographic Data Centre.

Synthesis of thyminyl stilbazoles

(E)-5-Methyl-1-(4-(2-(pyridin-4-yl)vinyl)benzyl)pyrimidine -2,4(1H,3H)-dione (VBT-4Pyr, 1): Vinylbenzylthymine (1.30 g, 6.33 mmol), NaOAc (0.78 g, 9.51 mmol), tri(*o*-tolyl)phosphine (P(*o*-tol)$_3$) (0.44 g, 1.43 mmol), Pd(OAc)$_2$ (80 mg, 0.36 mmol), and 4-bromopyridine hydrochloride (0.62 g, 3.19 mmol) were suspended in 20 mL DMF in a 35 mL microwave vial. The vial was capped and flushed with dry N_2 for 5 minutes, prior to microwave irradiation. The reaction temperature was raised from 70˚C to 140˚C, in increments of 10˚C.min^{-1} and the temperature was then maintained at 140˚C for 1 h. The cooled reaction mixture was filtered through a Celite plug, and the plug was thrice washed with 15 mL portions of DMF. The filtrate was evaporated to yield a yellow-orange gum. CH_2Cl_2 (6 - 10 mL) was used to precipitate the compound, **1**. The precipitate was collected by filtration, washed with further portions of CH_2Cl_2, and finally recrystallized from MeCN.

Yield: 0.75 g, 75%. M.p.: 261-263.1°C. HRMS (ESI)$^+$: m/z 320.1396 (M+H)$^+$ (requires m/z 320.1399). ^{1}H NMR: (400 MHz, D_6-DMSO) δ 1.76 (d, J = 0.8 Hz, 3H, C5-CH_3), 4.85 (s, 2H, N1-CH_2), 7.23 (d, J = 16.4 Hz, 1H, alkene CH), 7.33 (d, J = 8.00 Hz, 2H, Ar CH), 7.53 (d, J = 16.4 Hz, 1H, alkene CH), 7.55 (dd, J = 4.4, 1.6 Hz, 2H, Pyr CH), 7.61-7.67 (m, 3H Ar CH, C6H), 8.54 (dd, J = 4.8, 1.6 Hz, 2H, Pyr CH), 11.3 (br. s, 1H, NH). ^{13}C NMR (100 MHz, D_6-DMSO): δ_C 11.78 (C5-<u>C</u>H$_3$), 49.9 (N1-CH_2), 109.1 (C5), 120.9 (Pyr CH), 126.1 (alkene CH), 127.5 (Ar CH), 128.0 (Ar CH), 132.5 (alkene CH), 135.6 (Ar C), 137.5 (Ar C), 141.3 (C6), 144.2 (Pyr C), 150.1 (Pyr CH), 151.03 (C2), 164.25 (C4). Selected IR bands (ATR, cm^{-1}): 2955 m, 1734 m, 1696 s, 1667 s, 1600 m, 1443 m, 1408 m, 1376 m, 1346 m, 1246 m, 1201 m, 1080 w, 1003 m, 967 m, 953 m, 890 m, 842 m, 820 m, 764 m.

(E)-5-Methyl-1-(4-(2-(pyridin-3-yl)vinyl)benzyl)pyrimidine -2,4(1H,3H)-dione (VBT-3Pyr, 2): VBT-3Pyr (**2**) was prepared using a similar procedure to that used for the preparation of VBT-4Pyr (**1**) except the following reagents and quantities were used: Vinylbenzylthymine (1.30 g, 5.37 mmol), NaOAc (0.88 g, 10.7 mmol), P(*o*-tol)$_3$ (0.44 g, 1.45 mmol), Pd(OAc)$_2$ (80 mg, 0.36 mmol), and 3-bromopyridine (0.57 g, 3.58 mmol).

Yield: 0.62 g, 55%. M.p.: 245-247.3°C. HRMS(ESI)$^+$: m/z 320.1396 (M+H)$^+$ (requires m/z 320.1399). ^{1}H NMR : (400 MHz, D_6-DMSO) δ 1.76 (d, J = 1.2 Hz, 3H, C5-CH_3), 4.85 (s, 2H, N1-CH_2), 7.24-7.41 (m, 5H, 2 Ar CH, 1 Pyr CH, 2 alkene CH), 7.61 (d, J = 8.0 Hz, 2H, Ar CH), 7.63 (d, J = 1.2 Hz, 1H, C6H), 8.04 (td, J = 8.0 Hz, 1H, Pyr CH), 8.45 (dd, J = 4.8, 1.4 Hz, 1H, Pyr CH), 8.76 (d, J = 2.0 Hz, 1H, Pyr CH), 11.32 (br. s, 1H, N3H). ^{13}C NMR (100 MHz, D_6-DMSO): δ_C 11.84 (C5-<u>C</u>H$_3$), 49.77 (N1-CH_2), 108.98 (C5), 120.76 (Pyr CH), 126.03 (alkene CH), 127.22 (Ar CH), 127.84 (Ar CH), 132.39 (alkene CH), 135.50 (Pyr C), 137.35 (Ar C), 137.61 (Pyr CH), 141.16 (C6H), 144.07 (Ar C), 149.92 (Pyr CH), 150.92 (C2), 164.15 (C4). Selected IR bands (ATR, cm^{-1}): 3404 m, 2955 m, 1733 m, 1696 s, 1663 s, 1637 s, 1509 m, 1459 m, 1427 m, 1382 m, 1352 m, 1197 s, 1046 m, 999 w, 947 w, 819 w, 766 m.

(E)-3,5-Dimethyl-1-(4-(2-(pyridin-4-yl)vinyl)benzyl)-pyrimidine-2,4(1H,3H)-dione (VMT-4Pyr, 3): VMT-4Pyr (**3**) was prepared using a similar procedure to that used for the preparation of VBT-4Pyr (**1**) except a modified workup procedure was employed, and the following reagents and quantities were used: methylated vinylbenzylthymine (1.17 g, 4.54 mmol), 2-*tert*-butyl-4-methylphenol (5 mg, 0.03 mmol), NaOAc (0.74 g, 9.10 mmol), P(*o*-tol)$_3$ (0.23 g, 0.78 mmol), Pd(OAc)$_2$ (70 mg, 0.30 mmol), and 4-bromopyridine hydrochloride (0.59 g, 3.03 mmol). After filtration of the reaction mixture through Celite as described previously, the DMF was evaporated to give a yellow-orange oil which was taken up in 10% sodium hydroxide (25 mL) and extracted thrice with CH_2Cl_2 (50 mL portions). The organic phase was dried over $MgSO_4$ and the solvent was evaporated from the filtrate under reduced pressure. The residue was taken up in CH_2Cl_2 (5 mL) and the product was precipitated upon addition of hexane (100 mL). The whole sample was recrystallised by adding a boiling CH_2Cl_2 (3 mL) solution to boiling hexane (25 mL). The resulting milky suspension was heated for a further 5 min. Upon cooling and slow evaporation, single crystals of VBMT-4Pyr (**3**) were obtained and isolated by filtration.

Yield: 0.32 g, 32%. M.p.: 179.0-184.3°C. HRMS (ESI)$^+$: m/z 334.1553 (M+H)$^+$ (requires m/z 334.1556). ^{1}H NMR: (400 MHz, $CDCl_3$) δ 1.94 (d, J = 1.2 Hz, 3H, C5-CH_3), 3.41 (s, 3H, N3-CH_3), 4.95 (s, 2H, N1-CH_2), 7.02 (d, J = 0.8 Hz, 1H, C6H), 7.03 (d, J = 16.4 Hz, 1H, alkene CH), 7.35 (m, 5H, 2 Ar CH, 2 Pyr CH, 1 alkene CH), 7.55 (d, J = 8.4 Hz, 2H, Ar CH), 8.60 (d, J = 5.6 Hz, 2H, 2 Pyr CH). ^{13}C NMR (100 MHz, $CDCl_3$): δ_C 13.10 (C5-*CH$_3$*), 28.13 (N3-CH_3), 51.8 (N1-CH_2), 110.4 (C5), 120.9

(Pyr CH), 126.7 (Ar CH), 127.6 (alkene CH), 128.4 (Ar CH), 132.3 (alkene CH), 136.2 (Ar C), 136.3 (Ar C), 137.5 (C6H), 144.4 (Pyr C), 150.1 (Pyr CH), 151.9 (C2), 163.8 (C4). Selected IR bands (ATR, cm^{-1}): 3451 w, 3084 w, 2955 m, 1733 m, 1696 m, 1662 s, 1637 s, 1509 m, 1459 s, 1380 s, 1259 m, 1198 s, 1047 m, 999 w, 946 w, 843 w, 765 m.

(E)-3,5-Dimethyl-1-(4-(2-(pyridin-3-yl)vinyl)benzyl)-pyrimidine-2,4(1H,3H)-dione (VMT-3Pyr, 4): VMT-3Pyr (**4**) was prepared using a similar procedure to that used for the preparation of VBT-4Pyr (**1**) except the following reagents and quantities were used: methylated vinylbenzylthymine (1.17 g, 4.54 mmol), 2-*tert*-butyl-4-methylphenol (5 mg, 0.03 mmol), NaOAc (0.74 g, 9.1 mmol), P(*o*-tol)$_3$ (0.37 g, 1.21 mmol), $Pd(OAc)_2$ (70 mg, 0.30 mmol), and 3-bromopyridine (0.48 g, 3.03 mmol).

Yield: 0.07 g, 7%. M.p.: 182.8-185.2°C (dec.). HRMS (ESI^+): m/z 334.1553 $(M+H)^+$ (requires m/z 334.1556). ^{1}H NMR : (400 MHz, $CDCl_3$) δ 1.94 (d, J = 0.8 Hz, 3H, C5-CH_3), 3.41 (s, 3H, *N*3-CH_3), 4.95 (s, 2H, *N*1-CH_2), 7.02 (d, J = 0.8 Hz, 1H, C6H), 7.13 (dd, J = 16.4 Hz, 2H, alkene CH), 7.31-7.35 (m, 3H, 2 Ar CH, 1 Pyr CH), 7.55 (d, J = 8.2 Hz, 2H, Ar CH), 7.87 (td, J = 8.0, 1.8 Hz, 1H, Pyr CH), 8.52 (dd, J = 4.4, 0.8 Hz, 1H, Pyr CH), 8.75 (d, J = 1.6 Hz, 1H, Pyr CH). ^{13}C NMR (100 MHz, $CDCl_3$): δ_C 13.1 (C5-CH_3), 28.2 (*N*3-CH_3), 51.8 (*N*1-CH_2), 110.3 (C5), 123.7 (Pyr CH), 125.6 (alkene CH), 127.3 (Ar CH), 128.4 (Ar CH), 130.1 (alkene CH), 133.0 (Pyr C), 133.0 (Pyr. CH), 135.6 (Ar C), 136.8 (Ar C), 137.6 (C6H), 148.3 (Pyr CH), 148.4 (Pyr CH), 151.9 (C2), 163.8 (C4). Selected IR bands (ATR, cm^{-1}): 3029 w, 2985 w, 2954 w, 2926 w, 1665 s, 1640 s, 1510 w, 1471 m, 1360 m, 1334 m, 1258 w, 1201 m, 1111 w, 1023 w, 963 m, 952 m, 928 w, 829 m, 802 m, 761 s, 703 s.

1,1'-(((2,4-Di(pyridin-4-yl)cyclobutane-1,3-diyl)bis(4,1-phenylene))bis(methylene))bis(3,5-dimethylpyrimidine-2,4(1H,3H)-dione) (VMT-4Pyr photo-dimer, 5): The crystals of VMT-4Pyr (**3**) were spread in a thin layer in a petri-dish, and irradiated at 302 nm for a period of 17 h using a CL1000S UV-crosslinker lamp (UVP). The compound **5** was obtained in near quantitative yield as a yellow solid. Purification of the compound was performed by recrystallisation from MeOH/Acetone.

Yield: 96-98%. M.p.: 245-246°C. MS $(ESI)^+$: Calcd for $C_{22}H_{23}N_4O_8$: m/z 666.3; Found: m/z 667.3 $(M+H)^+$; 334.2 $(M+2H)^{2+}$. ^{1}H NMR (400 MHz, DMSO-d_6): δ_H 1.79 (d, J = 1.2 Hz, 6H, C5-CH_3), 3.17 (s, 6H, *N*3-CH_3), 4.55 (dd, J = 16.6 Hz, 6.8 Hz, 4H, cyclobut. CH), 4.79 (s, 4H, *N*1-CH_2), 7.17-7.27 (m, 12H, Pyr CH, Ar CH), 7.58 (d, J = 1.2 Hz, 2H, C6H), 8.45 (dd, J = 4.8 Hz, 1.6 Hz, 4H, Pyr H). ^{13}C NMR (D_6-DMSO): δ_C 12.8 (C5-CH_3), 29.6 (*N*3-CH_3), 48.0 (cyclobut. CH), 53.1 (*N*1-CH_2), 110.3 (C5), 123.8 (Pyr C), 127.7 (Ar C), 129.1 (Ar C), 134.1 (Ar C), 135.2 (Ar C), 138.4 (C6H), 152.2 (Pyr C), 155.4 (Pyr C), 155.6 (C2), 162.8 (C4). Selected IR bands (ATR, cm^{-1}): 3405 m, 3085 w, 2956 m, 1733 m, 1696 m, 1662 s, 1638 s, 1509 m, 1458 m, 1428 m, 1380 m, 1354 m, 1260 m, 1197 s, 1047 m, 999 w, 946 w, 842 w, 766 m.

Results and discussion

Synthesis of thyminyl stilbazoles

To synthesize thyminyl stilbazoles, we have used the Heck reaction of halo-pyridine substrates with vinylbenzyl thymine or methylated vinylbenzylthymine. Vinylbenzyl thymine and methylated vinylbenzylthymine have previously been used as a monomer in radical polymerisations, and various preparation procedures have already been described.[18-20] Using a literature procedure, vinylbenzyl thymine and methylated vinylbenzylthymine were synthesized in alkaline aqueous media by substitution of the N1 thyminyl hydrogen with vinylbenzyl chloride.[21] Four molecules, vinylbenzyl-thymine with 4-pyridine (VBT-4Pyr, **1**) and with 3-pyridine (VBT-3Pyr, **2**) and methylated vinylbenzylthymine with 4-pyridine (VMT-4Pyr, **3**) and with 3-pyridine (VMT-3Pyr, **4**) were synthesized using $Pd(OAc)_2$ as a catalyst with added phosphine ligand P(*o*-tol)$_3$). The products were obtained as solids that were spectroscopically consistent with the target compounds.

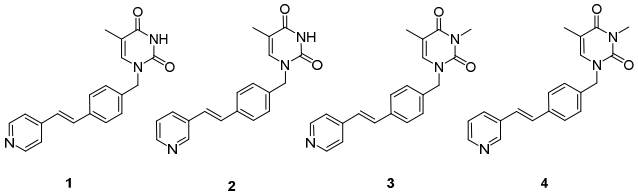

Figure 2. Synthesized thyminyl stilbazoles.

Photo-activity and crystal structure of thyminyl stilbazoles

Single crystals of VBT-4Pyr (**1**) were grown by slowly cooling a boiled MeCN solution. A portion of the resulting crystals (pale yellow needles) were collected by filtration and irradiated with 302 nm UV to test the solid-state photo-activity of the new compound. At the end of UV irradiation (17 h), the crystals had changed from a pale yellow to darker yellow colour. However, comparison of the ^{1}H-NMR spectra of irradiated and non-irradiated **1** samples did not reveal any changes, thereby indicating that photo-product formation had not occurred.

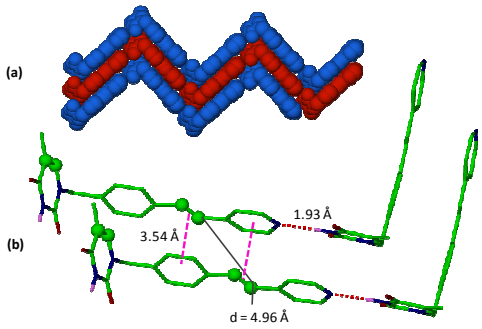

Figure 3. Crystal structure of VBT-4Pyr (**1**) (a) Packing diagram shows the herringbone-like pattern formed by stacking of the hydrogen bonded tape strands, (b) shows the N3H...N(pyr.) hydrogen bond and the relationship between proximity related pairs of **1**.

To ascertain the topochemical reasons for photo-stability of the sample, a crystal of **1** was subjected to analysis by SC-XRD on the MX1 beamline at the Australian Synchrotron. The crystal structure obtained is shown in **Figure 3**. Referring to the crystal structure, the main driving force for crystal packing was NH···N

hydrogen bonding between the thyminyl N3H of one molecule and the pyridyl nitrogen of another molecule. These N3H···N hydrogen bonds were 1.93 Å in length, and continued throughout the lattice to produce a1-dimensional hydrogen bonded tape. The hydrogen bonded tape structures then stacked on top of one another to give the overall herringbone-like structure shown in **Figure 3a**. The tightly stacked tape strands meant that parallel **1** molecules were separated by short distances (closest contact, 3.29 Å). As shown in **Figure 3b**, the tight packing of parallel **1** molecules was potentially stabilised by π-π interactions between the olefin and benzyl ring (3.54 Å), and the olefin and pyridyl ring (3.54 Å). Despite such close molecular packing however, the separation distance between the photo-dimerisable stilbazole olefins was 4.96 Å due to a molecular slip the length of the NH···N hydrogen bond. This distance was well outside the photo-activity constraints described by Schmidt,[6] and was probably the reason for photo-stability of the crystals.

Crystals of VBT-3Pyr (**2**) were grown from a hot ethanolic solution to yield a yellow crystalline solid. The crystals were screened for photo-activity by irradiating a sample with 302 nm UV light. Again, the crystals were photo-stable, as no changes were identified in the ^{1}H-NMR spectrum of the irradiated sample.

To explain the photo-stability of **2**, its crystal structure was determined, and is represented in **Figure 4**. As expected, changing the position of the pyridyl nitrogen from the 4- to 3-position did destabilise the imide···pyridine hydrogen bond. However, two new Watson and Crick style hydrogen bonds formed instead between the N3 hydrogens and the C4 carbonyls of adjacent thyminyl moieties (i.e N3H···O=C4; C4=O···HN3), as shown in **Figure 4**. The length of the hydrogen bonds was 1.92 Å. Compared with **1**, the Watson and Crick style hydrogen bonds in the **2** crystal altered the overall crystal structure substantially. Whereas infinite strands of hydrogen bonded molecules were observed in the **1** structure, the **2** structure formed discrete molecular pairs that were stabilised by the two hydrogen bonds between the thyminyl rings. Pairs of **2** molecules slip-stacked on top of one another to generate layers, but again the separation of the stilbazole olefins was too far for photo-dimerization to occur (4.87 Å).

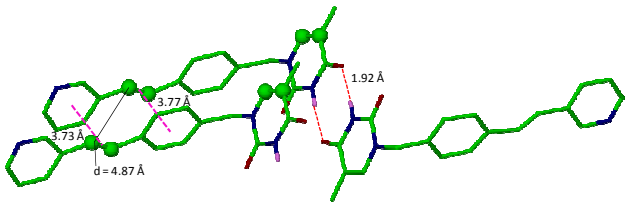

Figure 4. Crystal structure of VBT-3Pyr (**2**).

Crystals of each of VMT-4Pyr (**3**) and VMT-3Pyr (**4**) were grown by preparing boiling solutions of each compound in a few millilitres of CH_2Cl_2. Boiling hexane (25 mL) was then added to the solution to form a milky suspension, which was heated and stirred for further 5 minutes before slowly cooling. On cooling, crystals suitable for analysis by SC-XRD were isolated by filtration. The crystal structures corresponding to **4** and **3** are shown in **Figure 5** and **Figure 6**, respectively.

In the VMT-3Pyr (**4**) crystal structure in **Figure 5**, the main driving force for crystal packing was π-π interactions. Molecules of **4** stacked on top of one another to produce nearly parallel molecular pairs that were closely associated by distances of around 3.0 Å. Again, molecules of **4** slip-stacked on top of one another to produce displaced pairs, as shown in **Figure 5**. This arrangement appeared to be stabilised by π-π stacking interactions between the olefin···aryl (3.01 Å) and the olefin···pyridine (2.97 Å) moieties. The slipped molecular stacking meant that the stilbazole olefins were separated by too great a distance for them to be photoreactive toward [2π+2π]-cycloaddition (d = 4.40 Å). This finding was confirmed by irradiation of the compound and subsequent spectroscopic analysis of the sample using ^{1}H-NMR spectroscopy which indicated unchanged **4**.

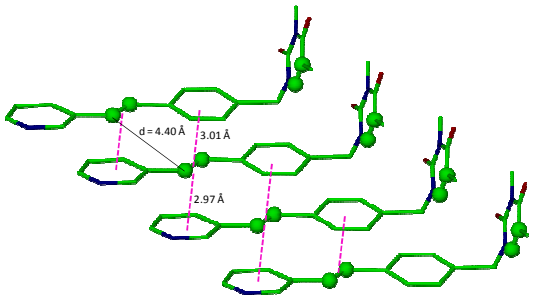

Figure 5. Crystal structure of VMT-3Pyr (**4**).

As shown in **Figure 6**, and in contrast with the previous structures that packed in head-to-head arrangements, VMT-4Pyr (**3**) molecules packed in a head-to-tail fashion with respect to the stilbazole moiety. This type of packing resulted in pairing of the stilbazole groups, and protrusion of the thyminyl rings at either end of the pair. The thyminyl rings of one stilbazole pair then associated with the protruding thyminyl rings of the next pair through trans-anti type π-π interactions to give the impression of molecular columns. These 'columns' packed to give the overall structure as shown in **Figure 6**.

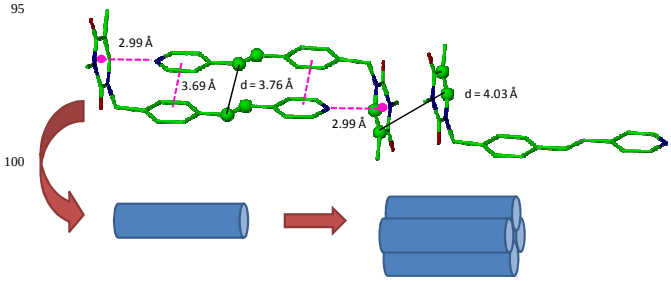

Figure 6. Crystal structure of VMT-4Pyr (**3**). Schematic representation of the molecules packing into "columns" that pack to give the overall structure.

Head-to-tail molecular pairing was apparently stabilised by the two aryl···pyridine (3.69 Å) π-π interactions and the olefin···olefin π-π interaction occurring at the stilbazole moieties. Collectively, these three weak interactions imposed parallel pairing of the stilbazole olefins, such that the stilbazole olefinic bonds were separated by a distance of 3.75 Å, which was suitable for photo-dimerization of the stilbazoles using the [2π+2π]-cycloaddition.

As stated above, the protruding thyminyl rings of the stilbazole pairs associated with those of the next pairs, which resulted in trans-anti type pairing and thus the reactive double bonds of the thyminyl rings were separated by a distance of 4.03 Å, also suitable for photo-dimerization by the [2π+2π]-cycloaddition reaction.

Photo-activity and crystal structure of thyminyl stilbazoles

An irradiated sample of the VMT-4Pyr (**3**) crystals (302 nm, 17 h) was subjected to UV-Vis and ^{1}H NMR spectroscopic analyses, which revealed that photo-dimerization occurred exclusively at the stilbazole moiety. The UV absorption spectra of **3** and the corresponding photo-product **5** are shown in **Figure 7**.

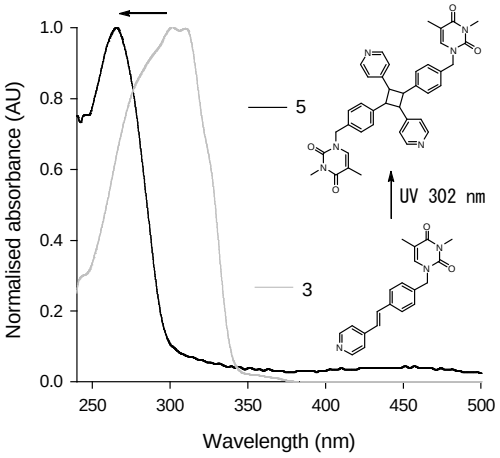

Figure 7. UV-Vis spectra obtained for $CHCl_3$ solutions of VMT-4Pyr (**3**) and the photo-product (**5**).

The UV absorption spectrum of **3** shows strong absorption at 302 nm which arises from the stilbazole portion of the molecule,[10] while the UV-Vis absorption spectrum of the photo-product **5** shows absorption at 266 nm (attributable to the thyminyl portion of the molecule). In the **3** spectrum, absorbance by the thyminyl moiety at 266 nm is saturated by the 302 nm stilbazole absorption. The disappearance of the 302 nm absorption band in the photo-product UV-Vis spectrum therefore indicates that the stilbazole olefin underwent photo-reaction upon irradiation, not the thyminyl olefin. Moreover, the ^{1}H-NMR spectrum of the photo-product of **3** revealed a multiplet at δ 4.45 ppm (in D_6-DMSO) arising from cyclobutane CH protons, while the doublet signal at δ 7.03 ppm (in $CDCl_3$) (from the stilbazole olefin in **3**) was absent in the spectrum of the photo-product **5**. There was no evidence of cyclobutane formation at the thyminyl moiety, since the signals for non-reacted thyminyl C5-CH3 and C6H could still be identified in the ^{1}H-NMR spectrum of the photo-product **5**, while the typical upfield shifts observed for the C5-CH3 protons of thyminyl cyclobutane derivatives were absent. GPC and MS analyses on the photo-product sample confirmed that a dimeric species was the exclusive photo-product. Considering the crystal structure of the starting material **3**, the photo-product was expected to be the head-to-tail stilbazole dimer **5**.

As previously mentioned, the crystal structure of **3** in **Figure 6** revealed that both the stilbazole olefins and thyminyl olefins were suitably aligned for photo-dimerisation by the [2π+2π]-cycloaddition reaction. It was therefore interesting to discover that only the stilbazole moiety underwent dimerisation to give stilbazole dimer **5**, and that none of the other possible products shown in **Figure 1** had formed. The thyminyl cyclobutane dimer in **Figure 1** would be the product of exclusive photo-reaction of the thyminyl olefins, while the polymer in **Figure 1** would result from photo-reaction at both the stilbazole olefins and the thyminyl olefins.

The UV-Vis spectrum of VMT-4Pyr (**3**) showed strong absorbance at 302 nm from the stilbazole moiety (which was also the wavelength used to synthesize **5**). Thus it was proposed that the 302 nm irradiation wavelength more specifically targeted photo-reaction at the stilbazole moiety rather than the thyminyl moiety. In order to determine whether changing the irradiation protocol could lead to a change in the photo-products obtained (in particular, generation of the photo-polymer or the thyminyl dimer, two further experiments were conducted. Firstly, a sample of **3** was irradiated with 302 nm UV light (17 h) to obtain the corresponding head-to-tail stilbazole cyclobutane photo-dimer (**5**), and then this sample was irradiated with 254 nm UV in an attempt to achieve photo-conversion at the thyminyl rings. Unfortunately, no further photo-reactions were observed upon comparison of the ^{1}H-NMR spectra before and after irradiation with 254 nm UV light. In a separate experiment, a fresh sample of crystalline **3** was directly irradiated with 254 nm UV. Again, only photo-dimerisation of the stilbazole olefins was observed (although it was incomplete after 17 h). From these two results, it did not appear that the photo-stability of the thyminyl olefin could be attributed to the irradiation wavelength utilised for the [2π+2π]-cycloaddition reaction. Instead, a number of structural factors were considered in order to explain the photo-stability of the thyminyl olefins in samples of **3** and **5**.

Firstly, it was possible that photo-reaction of the stilbazole olefins caused disruption of the "ideal" thyminyl ring packing observed in the **3** crystal structure, such that the thyminyl moieties no longer adopted suitable conformations for the [2π+2π]-cycloaddition reaction to occur at the thyminyl olefins. Only direct re-analysis of the irradiated **3** crystals by SC-XRD would provide definitive structural evidence for photo-induced changes to the thyminyl ring packing arrangement and this was not possible as the **3** crystals fractured during the photo-reactions. It should also be noted that for exclusive formation of the **5** stilbazole photo-dimers to occur during irradiation, it is necessary that the stilbazole olefins react preferentially. Referring to the crystal structure in **Figure 5**, the stilbazole olefins are separated by a shorter distance than the thyminyl olefins (3.76 Å versus 4.04 Å, respectively), which may help account for the observed photo-stability of the thyminyl olefins. Another possible reason for the photo-stability could be associated with the crowded packing around the thyminyl rings. As observed in the crystal structure of **3** in **Figure 5**, the pyridyl nitrogen atoms are in close proximity with the thyminyl ring centroids (2.99 Å) and the two rings produce an edge-to-face arrangement. Meanwhile, the thyminyl rings also form π-π stabilised trans-anti-type pairs. For the thyminyl olefins to undergo a [2π+2π]-cycloaddition reaction, the thyminyl rings would need to rotate slightly in order to achieve an overlap between the π-orbitals of the olefins. This type of motion, however, could potentially be blocked by the

pyridyl rings that are positioned in close proximity behind each thyminyl ring.

While it was not possible to directly analyse the "as-irradiated" **5** dimer sample by SC-XRD due to poor crystal integrity after irradiation, the crystal structure of **5** was eventually obtained by SC-XRD analysis of a recrystallized sample of the compound. As shown in **Figure 8**, the crystal structure obtained for stilbazole dimer **5** supports the previous spectroscopic identification of the photo-product as the head-to-tail stilbazole cyclobutane. For clarity, a schematic showing the configuration of substitutents around the cyclobutane is included in **Figure 8**.

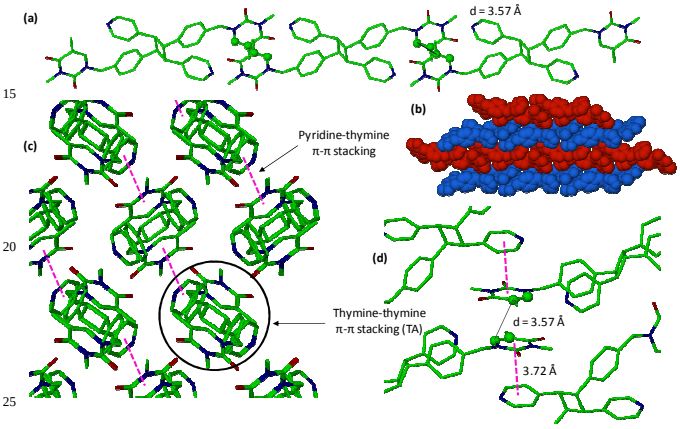

Figure 8. Crystal structure of dimer **5**. (a) Thyminyl alignment in a row of **5** molecules. (b) Packing diagram showing a stack of rows of **5** molecules. (c) View down the c-axis and down the rows of **5** molecules. Thymine-thymine π-π stacking stabilises the rows of **5** molecules, while stacking of the rows is stabilised by thymine-pyridine π-π interactions. (d) A closer view of the thymine-thymine and thymine-pyridine pairs.

In the crystal structure, molecules of **5** pack into rows which are potentially stabilised by trans-anti type thymine-thymine π-π stacking interactions (**Figure 8a**). The rows then stack to give the extended structure shown in **Figure 8b**. Close pyridine-thymine π-π stacking interactions appear to further stabilise the stacked structure (3.72 Å, see **Figure 8c, d**). Interestingly, the crystal structure of the **5** cyclobutane compound shows that the distance between the olefins of proximity-related thyminyl units is only 3.57 Å, yet irradiation of the recrystallised **5** sample (302 nm) did not afford any new photo-products. Photo-stability of the thyminyl olefins was again attributed to crowded packing around the thyminyl rings (**Figure 8d**). For the thyminyl olefins to undergo a [2π+2π]-cycloaddition reaction, the thyminyl rings would need to rotate slightly in order for the π-orbitals of the olefins to interact. In the **5** structure, this type of motion would probably be inhibited by the thymine-pyridine sandwiches.

Conclusions

Four thyminyl stilbazoles were synthesized using the Heck reaction and were each examined crystallographically. The crystal structures of the compounds **1** and **2**, each possessed a free imide N3H which underwent intermolecular hydrogen bonding interactions and contributed to the slipped stacking of the stilbazole portions of the molecules leading to large olefinic separation distances (4.99 and 4.87 Å, respectively). When the imide was methylated (compounds **3** and **4**) this hydrogen bonding site was eliminated, which facilitated closer packing of the stilbazole olefins (3.76 and 4.40 Å, respectively).

Only crystals of the VMT-4Pyr (**3**) underwent [2+2]-cycloaddition to give a cyclobutane dimer (**5**). ^{1}H-NMR and UV-Vis spectroscopic analyses were used to classify the photo-product as the head-to-tail stilbazole cyclobutane dimer. A number of structural factors were considered in order to explain the photo-stability of the thyminyl olefins in crystal structures of **3** and **5**.

Acknowledgement

We thank Dr Craig Forsyth, Dr David Turner, and the Australian Synchrotron MX beamline staff for any help they have provided with the crystallographic experiments.

Notes and references

[a] *School of Chemistry, Monash University, VIC 3800, Australia*
Fax: +61-3-9905-8501; Tel: +61-3-9905-4600; E-mail: kei.saito@monash.edu

1. K. Biradha and R. Santra, Crystal engineering of topochemical solid state reactions, *Chem. Soc. Rev.*, 2013, **42**, 950-967.
2. A. Matsumoto, Reaction of 1,3-diene compounds in the crystalline state, *Top. Curr. Chem.*, 2005, **254**, 263-305.
3. P. Klán and J. Wirz, Chemistry of excited molecules, in *Photochemistry of Organic Compounds*, John Wiley & Sons, Ltd, 2009, pp. 227-453.
4. G. Kaur, P. Johnston and K. Saito, Photo-reversible reactions and their applications in polymeric systems, *Polym. Chem.*, 2014, **5**, 2171-2186.
5. A. Sergeiko, V. V. Poroikov, L. O. Hanu and V. M. Dembitsky, Cyclobutane-containing alkaloids: Origin, synthesis, and biological activities, *Open Med. Chem. J.*, 2008, **2**, 26-37.
6. G. M. J. Schmidt, Photodimerizations in the solid state, *Pure Appl. Chem.*, 1971, **27**, 647-678.
7. K. Gnanaguru, N. Ramasubbu, K. Venkatesan and V. Ramamurthy, A study on the photochemical dimerization of coumarins in the solid state, *J. Org. Chem.*, 1985, **50**, 2337-2346.
8. H. Kashida, T. Doi, T. Sakakibara, T. Hayashi and H. Asanuma, p-stilbazole moieties as artifical base pair for photo-cross-linking of DNA duplex, *J. Am. Chem. Soc.*, 2013, **135**, 7960-7966.
9. M. Pattabiraman, A. Natarajan, R. Kaliappan, J. T. Mague and V. Ramamurthy, Template directed photodimerization of trans-1,2-bis(n-pyridyl)ethylenes and stilbazoles in water, *Chem. Commun.*, 2005, 4542-4544.
10. B. Mondal, B. Captain, and V. Ramamurthy, Photodimerization of HCl salts of azastilbenes in the solid state, *Photochem. Photobiol. Sci.*, 2011, **10**, 891-894.
11. D. Bučar, A. Sen, S. V. Santhana Mariappana and L. R. MacGillivray, A [2+2] cross-photodimerisation of photostable olefinsvia a three-component cocrystal solid solution, *Chem. Commun.*, 2012, **48**, 1790-1792.
12. E. Elacqua, R. C. Laird, R and L. R. MacGillivray, Templated [2 + 2] photodimerizations in the solid state, in *Supramolecular Chemistry: From Molecules to Nanomaterials*, eds. P. A. Gale and J. W. Steed, John Wiley & Sons, Ltd, 2012, **6**, 3153-3165.
13. J. Cadet and P. Vigny, The photochemistry of nucleic acids, in *Bioorganic Photochemistry*, ed. H. Morrison, John Wiley & Sons, Ltd, 1990, **1**, 1-272.
14. P. Johnston, C. Braybrook and K. Saito, Topochemical photo-reversible polymerization of a bioinspired monomer and its recovery and repolymerization after photo-depolymerization, *Chem. Sci.*, 2012, **3**, 2301-2306.

15. P. Johnston, E. I. Izagorodina and K. Saito, The interplay between hydrogen bonding and π-π stacking interactions in the crystal packing of N1-thyminyl derivatives, and implications to the photo-chemical [2π+2π]-cycloaddition of thyminyl compounds, *Photochem. Photobiol. Sci*., 2012, **11**, 1938-1951.
16. J. Cadet, S. Courdavault, J. L. Ravanat, T. Douki, UVB and UVA radiation-mediated damage to isolated and cellular DNA, *Pure Appl. Chem*,. 2005, **77**, 947-961.
17. R. B. Setlow, Repair deficient human disorder and cancer, *Nature*, 1978, **271**, 713-717.
18. D. M. Martino, D. Reyna, D. A. Estenoz, S. Trakhtenberg, J. C. Warner, Photosensitization of bioinspired thymine-containing polymers, *J. Phys. Chem. A*, 2008, **112**, 4786-4792.
19. R. McHale, J.P. Patterson, P.B. Zetterlund, and R.K. O'Reilly, Biomimetic radical polymerization via cooperative assembly of segregating templates, *Nature Chem*., 2012, **4**, 491-497.
20. J. E. Puskas, Y. Dahman, A. Margaritis, and M. Cunningham, Novel thymine-functionalized polystyrenes for applications in biotechnology. 2. adsorption of model proteins, *Biomacromolecules*, 2004, **5**, 1412-1421
21. C. M. Cheng, M. I. Egbe, J. M. Grasshoff, D. J. Guarrera, R. P. Pai, J. C. Warner and L. D. Taylor, Synthesis of 1-(vinylbenzyl)thymine, a novel, versatile multi-functional monomer, *J. Polym. Sci., Part A: Polym. Chem*. 1995, **33**, 2515-2519.